

This is the peer reviewed version of the following article: Liu S-P, Wipfler B & Beutel RG (2017) The unique locomotor apparatus of whirligig beetles of the tribe Orectochilini (Gyrinidae, Coleoptera). Journal of Systematic Research and Evolutionary Biology 56(2) 196-208, which has been published in final form at <https://doi.org/10.1111/jzs.12195>. This article may be used for non-commercial purposes in accordance with Wiley Terms and Conditions for Use of Self-Archived Versions.

1 **The unique locomotor apparatus of whirligig beetles of the tribe Orectochilini (Gyrinidae,**
2 **Coleoptera)**

3

4 **Si-Pei Liu¹, Benjamin Wipfler¹ and Rolf G. Beutel¹**

5

6 ¹*Institut für Spezielle Zoologie und Evolutionsbiologie mit Phyletischem Museum, Friedrich-*
7 *Schiller-Universität Jena, Jena*

8 *Corresponding author: Rolf G. Beutel (rolf.beutel@uni-jena.de)*

9 *Contributing authors: Si-Pei Liu (sipei.liu@uni-jena.de), Benjamin Wipfler*
10 *(benjamin.wipfler@uni-jena.de)*

11

12 **Abstract**

13 Whirligig beetles, which are known for their rapid gliding on the water surface, have evolved
14 a unique locomotor apparatus. External and internal thoracic structures of *Orectochilus villosus*
15 (Orectochilini) are described in detail and documented with micro-computed tomography,
16 computer based 3D reconstructions, and scanning electronic microscopy (SEM). The results
17 are compared with conditions found in other genera of Gyrinidae and other groups of
18 Coleoptera. The focus is on structures linked with locomotion, especially on the unusual flight
19 apparatus, which differs strongly from that of other beetles. As in other Orectochilini, the
20 prothorax of *Orectochilus* displays characters typical for Gyrinidae, with triangular procoxae
21 and fore legs transformed into elongated, sexually dimorphic grasping devices. The
22 musculature of this segment is similar to the pattern found in other Coleoptera. Similar to all
23 other extant Gyrinidae, the mesothorax is characterized by an extensive and flat mesoventrite,
24 suitable for gliding on the water surface. As in Heterogyrinae and the other Gyrininae, the
25 pterothoracic legs are transformed into paddle-like structures, enabling the beetles to move with
26 high speed on the surface film. The musculature of the mesothorax is reduced compared to
27 other Coleoptera, but similar to what is found in the other Gyrininae. The metathoracic skeleton
28 and musculature are simplified in Orectochilini compared to other Gyrininae and other groups
29 of Coleoptera. In *O. villosus* only 10 metathoracic muscles are preserved. Thirty-six are present
30 in an archostematan beetle, a condition probably close to the coleopteran groundplan. The
31 metathoracic dorsal longitudinal bundles are absent in Gyrininae, muscles that play a role as
32 indirect flight muscles in most other neopteran insects. The rest of the posteromotoric flight
33 apparatus is distinctly modified, with a limited number of skeletomuscular elements taking over
34 more than one function, i.e. leg movements and flight. The large muscle **M84** (IIIIdvm7) M.

35 noto-trochanteralis, for instance, functions as dominant wing levator, but is also responsible for
36 the powerful and rapid backstroke of the hind legs. The presence of this muscle is a
37 synapomorphy of Heterogyrinae and Gyriminae. The narrow metafurca in the latter group is
38 likely linked to its large size. The elytra likely contribute to the control of the flight of the beetle,
39 whereas they shield and inhibit the flight apparatus during swimming.

40

41 **Keywords:** Gyrimidae – *Orectochilus* – thorax – morphology – locomotor apparatus

42

43 **1. Introduction**

44 Whirligig beetles or Gyrimidae are known for swimming rapidly in circles on the water surface,
45 usually forming groups of several dozens or thousands of individuals (Bott 1928; Omer-Cooper
46 1934; Larsén 1966). According to Nachtigall (1961) their swimming apparatus is the most
47 efficient in the entire animal kingdom. The habitat with small arthropods caught in the surface
48 film was referred to as a “world of the dead and the dying” (Omer-Cooper 1934). The unusual
49 life habits of whirligig beetles are linked with a series of autapomorphies, including the
50 subdivided compound eyes and the antennae with fringes of setae on the pedicellus registering
51 movements of the water surface (e.g. Larsén 1966). The systematic position of the family within
52 the suborder Adephaga is not fully settled (e.g. McKenna et al. 2015). However, a sistergroup
53 relationship with all other adephagan families appears most likely, supported by morphological
54 characters (Beutel and Roughley 1988; Beutel, et al. 2013) and also by a recent molecular study
55 (Baca et al. 2017).

56 A comprehensive morphological study on the locomotor organs of Gyrimidae was
57 published by Larsén (1966), together with the thoracic morphology of 54 species in the
58 suborders Adephaga and Polyphaga. However, the work of Larsén (1966) was exclusively
59 based on dissections and focused on the species *Gyrinus marinus* Gyllenhal, 1808 (Gyrinini).
60 At that time, the gyrimid key taxon *Spanglerogyrus albiventris* Folkerts, 1979 and the
61 sistergroup of all the remaining genera was unknown. Besides this, no information on the
62 thoracic morphology of the plesiomorphic suborder Archostemata was available (Baehr 1975;
63 Friedrich et al. 2009).

64 In this study we focus on the tribe Orectochilini, which includes the genera *Gyretes*,
65 *Orectogyrus*, *Orectochilus* and *Patrus* (formerly a subgenus of *Orectochilus*; Miller and
66 Bergsten 2012). It is the subgroup with the most advanced features in this family according to
67 phylogenetic analyses of Gyrimidae (Larsén 1966; Beutel 1989a, b, 1990; Miller and Bergsten
68 2012). It cannot be excluded that some flightless species occur in Orectochilini (Larsén 1954).

69 However, there are records indicating that members of different genera of this tribe have
70 retained their flight capacity (Larsén 1966; Ochs 1966; Brinck 1982), including the one in the
71 focus of this study, *Orectochilus villosus* (Müller, 1776). The thoracic morphology of this
72 species is described in detail and documented using μ -CT data, computer based 3D
73 reconstructions and scanning electronic microscopy (SEM). The locomotor organs are
74 discussed from evolutionary and functional perspectives, especially the flight apparatus, which
75 is characterized by a distinctly modified skeleto-muscular apparatus compared to beetles of
76 other families or representatives of other groups of Neoptera (Larsén 1966; Brodsky 1994).

77

78 **2. Materials and Methods**

79 **2.1. Materials**

80 *Orectochilus villosus* (Müller, 1776), fixed in FAE (formaldehyde-acetic acid-ethanol) and
81 stored in ethanol, collected in the Saale river, 8 Km south of Jena (Thuringia, Germany).

82 *Heterogyrus milloti* Legros, 1953 (Heterogyrinae; MILLER & BERGSTEN 2012), fixed and stored
83 in 97% ethanol; collected at Fianarantsoa, small stream ~8km W Ranomofana, Ranomofana
84 NP, Madagascar, 21° 14.992' S 47° 24.332' E, 2 November 2014, Miller, Gustafson and
85 Bergsten.

86 Additional morphological data were extracted from the literature (Larsén 1954, 1966;
87 Beutel 1989a, b, 1990; Friedrich et al. 2009).

88

89 **2.2. Synchrotron radiation based micro-computed tomography (SR- μ CT)**

90 One specimen was dehydrated in an ethanol series and dried at the critical point (EmiTech K850
91 Critical Point Dryer). It was scanned in a small Eppendorf tube at Beamline BW2 of German
92 Electron Synchrotron Facility (DESY, Hamburg) using a stable low photon energy beam (8
93 kVP) and absorption contrast.

94

95 **2.3. Computer based 3D-reconstruction**

96 Based on the μ CT-image stack the thoracic segments of *O. villosus* were reconstructed three-
97 dimensionally using FEI Amira 6.0. Segmented structures were exported as stacks of tiff files
98 into Volume Graphics VGStudiomax 2.0, which was used for volume rendering.

100 **2.4. Scanning electronic microscopy**

101 For the examination of external skeletal structures, a dried specimen was coated with gold
102 (EmiTech K500 sputter coater). Micrographs were taken with Philips XL 30 ESEM and
103 ResAlta Scandium software.

104

105 **2.5. Microscopic photography**

106 To document the coloration and general body shape, the specimens were photographed with
107 Keyence VH-Z20R.

108

109 **2.6. Line drawings**

110 Exposed body parts of the specimen were drawn with full lines, structures below other sclerites
111 with dotted lines. In Fig. 3 wings and legs were omitted, except basal elements. In Fig. 6 elytra
112 are omitted. The figures were drawn with a pencil based on microscopic observations (with a
113 camera lucida) or on 3D-reconstructions, scanned and finally completed with Adobe Illustrator
114 CC.

115

116 **2.7. Measurements**

117 Measurements were taken from digital photographs, SEM micrographs, line drawings and 3D-
118 reconstruction according to respective scale bars. The original scale bars can be accurate to
119 0.001 mm. Considering the calculation error, we kept the accuracy to 0.01 mm. We consistently
120 chose the longest portion in each dimension for measurement (e.g. ventrite of the mesothorax).

121

122 **2.8. Terminology**

123 The terminology for the thoracic skeleton was adopted from Friedrich et al. (2008) and Larsén
124 (1966). Muscle names of both Larsén (1954) and Friedrich and Beutel (2008) are used for easy
125 comparison with other coleopteran taxa. Both studies were also used in the context of functional
126 interpretations of thoracic structures. Basisubcostale (bsc) as a significant structure during wing
127 stroke is also adopted from Brodsky (1994).

128

129 **Abbreviations:**

130 1/2/3ax – first/second/third axillary sclerite; aest2/3 – mes-/metanepisternum; alc – alacrista;
131 anp – anterior notal process; ba3 – metabasalare; bsc – basisubcostale; cx1/2/3 – pro-/meso-

132 /metacoxa; dis – discrimen; el – elytron; elap – articulatory process of elytron; ep2/3 –
133 mes/metepimeron; ep11 – proepipleuron; fem1/2/3 – pro-/meso-/metafemur; fu1/2/3 – pro-
134 /meso-/metafurca; hw – hind wing; fup – profurcal process; mnp – median notal process; nt1 –
135 pronotum; ph1/2 – pro-/mesophragma; pl1 – propleuron; pls2/3 – meso-/metapleural suture;
136 pn3 – metapostnotum; pnp – posterior notal process; prsc – prealar sclerite; pwp3 –
137 metathoracic pleural wing process; sc2/3 – meso-/metascutum; scl2/3 – meso-/metascutellum;
138 scsh – mesoscutellar shield; se – spatulate setae; spi2 – mesothoracic spiracle; su3 –
139 metasubalare; tar1/2/3 – pro-/meso-/metatarsus; tib1/2/3 – pro-/meso-/metatibia; tr1/2/3 – pro-
140 /meso-/metatrochanter; v1/2/3 – pro-/meso-/metaventricle.

141

142 **3. Results**

143 **Thoracic morphology of *Orectochilus villosus***

144 **General appearance**

145 Body length: 9.65 mm, width: 3.83 mm, height: 2.86 mm (length : width : height ratio = 3.4 :
146 1.3 : 1.0). The thorax appears compact, stream-lined and laterally compressed, with a flat
147 ventral surface and a convex dorsal side. The pronoto-elytral angle is indistinct. The pronotal
148 and elytral surfaces (Fig. 1A) bear a dense vestiture of fine setae.

149

150 **3.1. Prothorax**

151 Length: 1.87 mm (pronotum), width: 3.21 mm (pronotum), height: 2.16 mm (length : width :
152 height ratio = 1.0 : 1.7 : 1.2). Cervical sclerites are missing. The head and prothorax are
153 connected by a cervical membrane, which is not visible externally. A dense pubescence is
154 present on the entire pronotal surface. The anterior and posterior margins of the convex
155 pronotum (nt1: Figs. 1A, C; 3C; 5A) are not distinctly extended. The anterior pronotal area
156 covers the occipital region of the head and appears almost merged with it. The anterior pronotal
157 margin is very finely serrated. The proepipleuron (ep11: Figs. 1B; 3C; 5A) is narrow as in the
158 other *Orectochilini* (Larsén 1966). The propleuron (pl1: Figs. 1B; 3C; 5A) is delimited by a
159 suture extending obliquely from the antero-ventral margin of the epipleuron to the prothoracic
160 pleuro-coxal joint. The internalized crytopleura are extended mesad and fused with the
161 pronotum, only leaving a narrow tergal region for muscle attachment. This is a character shared
162 in *Orectochilini* and *Enhydrini* (Larsén 1966; Baehr 1979). The posterior wall (Fig. 3C) of the
163 prothorax is formed by the posterior area of pronotum, the posterolateral epipleural area and
164 the transverse concave ventral propleural lobe. The posterior pronotum (nt1: Fig. 3C) is narrow
165 in *O. villosus*, but even narrower in the other *Orectochilini* (Larsén 1966). The line separating

166 the epipleural and propleural elements of the posterior wall is indistinct, probably an
167 autapomorphy of Orectochilini (Larsén 1966). A projecting process bears a tuft of spatulate
168 setae (se: Fig. 3C), which form the proprioceptive sense organ located ventro-laterally on the
169 posterior segmental wall, as in other Orectochilini (Larsén 1966). The process is short and
170 rounded in *O. villosus* and *Gyretes*, but blunt in *Orectogyrus* (Larsén 1966). The proventrite
171 (Figs. 2A; 3C) is bulging medially as in *Orectogyrus* (Larsén 1966), gradually shortened
172 paramedially and laterally connected with the propleura. Medially it is divided by a distinct
173 median ridge, and another ridge is present along its posterior margin. The prosternal process is
174 reduced, not reaching between the procoxae. The profurca (fu1: Figs. 3C; 4C) bears a long
175 posterior arm, which is bent laterad and reaches deeply into the mesothoracic lumen as in other
176 Orectochilini and Enhydrini (Larsén 1966; Baehr 1979; Beutel 1989b). Anteriorly it bears a
177 vertically oriented profurcal process (fup: Fig. 3C).

178 The fore legs (Figs. 1B; 2A) are modified as elongate grasping devices. The procoxa (cx1:
179 Figs. 2A; 4A; 3C; 5A) is triangular and only slightly protruding. It lacks a ventral condyle
180 articulating with the prosternal process. The triangular protrochanter (tr1: Figs. 2A; 3C; 5A),
181 equipped with a group of setae ventrally, connects the procoxa with the elongate profemur
182 (fem1: Fig. 1B; 2A) (length: 1.83 mm, width: 0.46 mm; length : width ratio = 4.0 : 1.0). The
183 anterior profemoral margin bears a row of spines. The elongate protibia (tib1: Figs. 1B; 2A;
184 length: 1.47 mm, width: 0.26 mm; length : width = 5.7 : 1.0), basally narrow and distally
185 widening, bears a mesal comb of spines. Apical tibial spurs are missing. The sexually dimorphic
186 laterally compressed protarsus (tar1: Figs. 1B; 2A) is composed of five tightly connected
187 tarsomeres. The tarsal segments in males are equipped with a brush-like dense vestiture of
188 adhesive hairs with apical suckers. The distal tarsomere bears a pair of curved claws.

189 **Musculature** (Figs. 4; 5; see Table 1 for an overview of all muscles; abbreviations from
190 Friedrich and Beutel (2008) in brackets): **M1** (Idlm2) M. pronoti primum: O (= origin): antero-
191 median area of pronotum; I (= insertion): dorso-lateral area of occipitale. **M2** (Idlm1) M.
192 pronoti secundus, bent upwards: O: first phragma; I: dorso-lateral area of occipitale. **M3** (Idlm3)
193 M. pronoti tertius, bent upwards: O: first phragma; I: anterior pronotal margin. **M5** (IvIm3) M.
194 prosterni primus: O: basal area of profurca; I: ventro-lateral area of occipitale. **M6** (IvIm1) M.
195 prosterni secundus: O: profurcal process; I: ventral cervical membrane. **M7** (Idvm6) M.
196 dorsoventralis primus, broader on pronotum, narrowing towards occipitale: O: central area of
197 pronotum; I: ventro-lateral area of occipitale. **M10** (Idvm2/3) M. dorsoventralis quartus: O:
198 anterior margin of prosternum; I: dorso-lateral area of occipitale. **M11** (Idvm10) M.
199 dorsoventralis quintus, triangular muscle, narrower on mesoscutum; broadening towards

200 profurca: O: dorsal area of profurca; I: antero-lateral area of mesoscutum. **M13** (Itpm6) M.
 201 pronoto-mesepisternalis, broader on pronotum, narrowing towards mesanepisternum: O:
 202 central area of pronotum; I: intersegmental membrane anterior to mesanepisternum. **M14**
 203 (Idvm13) M. noto-trochantinalis, broader on pronotum, narrowing towards procoxa: O: antero-
 204 lateral area of pronotum; I: lateral procoxal rim. **M15** (Idvm16/17) M. noto-coxalis, broader on
 205 pronotum, narrowing towards procoxa: O: lateral area of pronotum; I: posterior procoxal rim.
 206 **M16** (Ipcm4) M. epimero-coxalis, broader on propleuron, narrowing towards procoxa: O:
 207 antero-dorsal area of propleuron; I: antero-lateral procoxal rim. **M20** (Ipcm8) M. pleura-
 208 trochanteralis, broader on prothoracic posterior wall, narrowing towards trochanter: O:
 209 prothoracic posterior wall; I: protrochanter. **M21** M. pleura-trochanteralis medialis, wide area
 210 of origin on procoxa, converging towards protrochanter: O: procoxal mesal wall; I:
 211 protrochanter. **M22** M. coxa-trochanteralis lateralis, at least two bundles, wide area of origin
 212 on procoxa, converging towards protrochanter: O: lateral procoxal wall; I: protrochanter.

213 The prothoracic muscles, especially those that attach to the cervical region and legs, are
 214 similar to those of the other examined species of Gyrinidae or other groups of Coleoptera
 215 (Larsén 1966; Baehr 1975; Beutel 1989b; Friedrich and Beutel 2006; Friedrich et al. 2009). The
 216 modifications compared with the general coleopteran muscular pattern reported by Larsén
 217 (1966: table II) and Beutel and Haas (2000: appendix IV) are the following: **M4** (Idlm5) M.
 218 pronoti quartus, **M8** (Idvm8) M. dorsoventralis secundus, **M9** (Idvm5) M. dorsoventralis tertius,
 219 **M12** (Itpm3?) M. pronoto-pleuralis, **M17** (Ipcm8) M. epimero-coxalis, **M18** (Iscm1) M. sterno-
 220 coxalis and **M19** (Iscm2) M. furca-coxalis are absent. The origin of **M1** (Idlm2) M. pronoti
 221 primum is shifted anterad. The origin of **M7** (Idvm6) M. dorsoventralis primus is shifted mesad.
 222 The original area of one subcomponent of **M15** (Idvm16/17) M. noto-coxalis is transverse and
 223 shifted to the postero-lateral region of the pronotum.

224

225 **3.2. Mesothorax**

226 Length 1.62 mm (mesoventrite + mesocoxa), width 3.48 mm (mesoventrite), height 1.76 mm
 227 (from mesoscutellar shield to mesoventrite, without elytra) (length : width : height ratio = 1.0 :
 228 2.1 : 1.1). A flat median concavity is present at the anterior margin of the mesoscutum (sc2:
 229 Fig. 3A) and both sides of the sclerite are protruding anteriorly. Paired, distally rounded
 230 processes extending postero-ventrad from the anterior concavity form the prophragma (ph1:
 231 Fig. 4C) in *O. villosus*. It is a single and apically truncated structure in *Orectogyrus* and also a
 232 single median lobe in a few species of *Gyretes*, whereas it is bilobed in the other Gyrinidae
 233 (Hatch 1926; Larsén 1966). The narrow sclerotized lateral edge of the mesoscutum lacks

234 recognizable notal processes. An axillary ligament connects it with the articular process of
235 the elytron (elap: Fig. 3A). The area between the mesoscutum and the posterior mesoscutellum
236 is unsclerotized, nearly membranous. The mesoscutellum (scl2: Fig. 3A) bears a sclerotized
237 triangular mesoscutellar shield (scsh: Fig. 3A) on its middle region, and its lateral parts are very
238 narrow. The mesopleuron is triangular. The mesanepisternum (aest2: Fig. 3D) bears a small
239 process on its dorsal margin, arguably a reduced mesobasalar. As in other Orectochilini, the
240 opening between the elytron and laterally expanded dorsal margin of the mesanepisternum is
241 narrow in *O. villosus* (Larsén 1966), an autapomorphy of the tribe (Beutel 1990). The ventral
242 mesanepisternal margin broadly connects with the dorso-lateral margin of the mesoventrite (v2:
243 Figs. 1B; 2A, B; 3D) and meets the lateral mesocoxal edge posteriorly. This ventral margin
244 forms an excavation for the profemora in the resting position. Postero-mesally the
245 mesanepisternum is adjacent to the narrow triangular mesepimeron (ep2: Fig. 3D), both
246 separated by the mesopleural suture (pls2: Fig. 3D). The mesokatepisternum is completely
247 fused with the main part of the mesoventrite, without a transverse ridge. Anteriorly the
248 mesoventrite forms a triangular process that bears two separate groups of setae, and postero-
249 mesally a discrimen (dis: Fig. 4A) is present protruding dorsad into the mesothoracic lumen.
250 The short but well-developed mesofurca (fu2: Fig. 4B) originates dorsally on the discrimen. It
251 bears a large apical disc for muscle attachment.

252 The mesocoxae are approximately triangular (cx2: Figs. 1B; 3D; 4A; 5A), medially
253 adjacent and diverging antero-laterally. The anterior edge is immovably attached to the
254 posterior margin of the mesoventrite. This is also the case in *Orectogyrus*, whereas a certain
255 movability is retained in *Gyretes* (Larsén 1966). The median line separating the round median
256 mesocoxal lamellae is anteriorly continuous with the discrimen. Antero-laterally an extensive
257 triangular apodeme is present for muscle attachment. Dorsally, the large trochanteral tendon for
258 muscle attachment expands to the region of the mesoventrite and the mesanepisternum.
259 Compared with generalized coleopteran walking legs, the distal parts of the middle legs are
260 strongly modified. The mesotrochanter (tr2: Figs. 1B; 2B; 3D; 4A; 5A) connects the mesocoxa
261 with the shortened, flattened and roughly triangular mesofemur (fem2: Figs. 1B; 2B; 5A; length:
262 0.77 mm, width: 0.45 mm; length : width ratio = 1.7 : 1.0). The mesofemur broadly connects
263 with the similarly broadened and flattened mesotibia (tib2: Figs. 1B; 2B; 5A; length: 0.75 mm,
264 width: 0.52 mm; length : width ratio = 1.4 : 1.0), which bears swimming lamellae antero-distally
265 and a row of spines posteriorly. The mesotarsus (tar2: Figs. 1B; 2B) inserts onto the apical
266 mesotibial margin. Its posterior margin is also equipped with swimming lamellae. The internal
267 walls of the mesotibiae and the proximal tarsomere are connected by the cuticular columnae,

268 as in the other Orectochilini and Enhydrini (Larsén 1966; Beutel 1990). The five tarsomeres
269 are flattened, together forming a fan-shaped structure. The distal margin of the tarsomere 4 is
270 bent dorsad, thus forming a shovel-like structure with the shape of the proximal 3 tarsomeres,
271 similar to the condition found in other Orectochilini and some Enhydrini (Larsén 1966; Beutel
272 1990). Tarsomere 5 is proximo-mesally connected with the tarsomere 4 and bears a pair of
273 curved claws apically.

274 The elytra (el: Figs. 1A, C; 5A) are posteriorly truncated and bear a dense vestiture of
275 short and thin setae, similar to the pronotal vestiture. The pubescent dorsal side of the body is
276 a diagnostic character of *Spanglerogyrus*, *Heterogyrus* and Orectochilini (Folkert 1979; Larsén
277 1966; Miller and Bergsten 2012). Elytral striae are absent. The glossula is present, as in the
278 other Orectochilini and Enhydrini (Larsén 1966; Beutel 1990).

279 **Musculature** (Figs. 4; 5; Table 1): **M28** (IIdlm1) M. mesonoti primus: O: first phragma;
280 I: second phragma. **M30** (IvIm7) M. mesosterni secundus: O: basal area of profurca; I:
281 mesofurcal arm. **M33** (IItpm2) M. noto-pleuralis: O: process of mesopleural ridge; I: dorso-
282 lateral area of intersegmental membrane between pro- and mesothorax. **M38** (Ispm5) M.
283 profurca-mesepisternalis: O: profurcal arm; I: anterior margin of mesanepisternum. **M40**
284 (IIdvm4/5) M. noto-coxalis, slightly broader medially: O: lateral area of mesoscutum; I:
285 postero-lateral mesocoxal rim. **M41** (IIpcm4) M. episterno-coxalis, broader on
286 mesanepisternum, narrowing towards mesocoxa: O: central area of mesanepisternum; I: antero-
287 lateral mesocoxal rim. **M43** (IIdvm6) M. coxa-subalaris, slightly broader medially: O:
288 membranous area between mesoscutum and mesanepisternum; I: postero-lateral mesocoxal rim.
289 **M46** (IIscm2) M. furca-coxalis posterior, broader on mesofurca, narrowing towards mesocoxa:
290 O: basal area of mesofurca; I: posterior mesocoxal rim. **M47** (IIdvm7) M. noto-trochanteralis:
291 O: mesoscutum; I: mesotrochanter. **M48** (IIpcm6) M. episterno-trochanteralis, triangular,
292 narrower on mesanepisternum, broadening towards mesotrochanter: O: dorsal area of
293 mesanepisternum; I: mesotrochanteral tendon. **M51** (?) M. sterno-trochanteralis: O:
294 invaginated area of mesoventrite; I: mesotrochanteral tendon. **M52** (IIscm6) M. furca-
295 trochanteralis, broader on mesofurca, narrowing towards mesocoxa: O: antero-ventral area of
296 mesofurcal arm; I: mesotrochanter. **M53** M. coxa-trochanteralis medialis, several bundles,
297 distributed over wide area of mesocoxa, converging towards mesotrochanter: O: mesocoxal
298 anterior rim and median wall; I: mesotrochanter. **M54** M. coxa-trochanteralis lateralis, two
299 bundles, the anterior one larger and stronger, the posterior one shorter: O: lateral mesocoxal
300 wall; I: mesotrochanter.

301 The muscular apparatus of the mesothorax comprises only 12 muscles (excl. **M53** and
302 **M54** as intrinsic mesocoxal muscles), compared to 25 in a more plesiomorphic pattern in other
303 groups of Adephaga and in Polyphaga (Larsén 1966; Beutel and Haas 1966) and 33 in the
304 archostematan *Tetraphalerus bruchi* Heller, 1913 (Friedrich et al. 2009). According to the
305 coleopteran musculature by Larsén (1954), **M29** (IIdlm2) *M. mesonoti secundus*, **M31** (Ivlm9)
306 *M. mesosterni secundus*, **M32** (IIdvm8) *M. dorsoventralis*, **M34** (IItpm10?) *M. noto-epimeralis*,
307 **M35** (IItpm10) *M. epimero-subalaris*, **M36** (IItpm7 & 9) *M. pleura-alaris*, **M37** (IIspm2) *M.*
308 *furca-pleuralis*, **M39** (IIdvm2) *M. noto-trochantinalis*, **M42** (IIpcm3) *M. episterno-coxalis*,
309 **M44** (IIscm1) *M. furca-coxalis anterior*, **M45** (IIscm4) *M. furca-coxalis lateralis*, **M49** (?) *M.*
310 *epimero-trochanteralis* and **M50** (IIpcm5) *M. trochantero-basalaris* are absent.

311

312 **3.3. Metathorax**

313 Length: 0.98 mm (metacoxa), width: 3.28 mm (paired metacoxae), height: 1.87 mm (from
314 central metascutal area to level of ventral mesocoxal surface) (without hind wings) (length :
315 width : height = 1.0 : 3.3 : 1.9. The propulsive force during flight is only created by the
316 metathorax as in the other beetles and in Strepsiptera (posteromotorism; e.g. Friedrich et al.
317 2010). The dorsal metathoracic parts are large compared with the corresponding mesothoracic
318 elements. The median portion of the metascutum (sc3: Fig. 3A, B, D) is short and lacks a
319 membranous area, but is widened laterally, as in other Orectochilini and Enhydrini (Hatch 1926;
320 Larsén 1966; Beutel 1990). The paired processes of the anterior metascutal margin bends
321 postero-ventrad into the thoracic lumen thus forming the mesophragma (ph2: Fig. 4D). Antero-
322 laterally the metascutum bears a very small sclerotized process, the metaprealar sclerite (prsc:
323 Fig. 3D), similar to a homologous structure in *Orectogyrus* (Larsén 1966). The alacristae (alc:
324 Fig. 3B) are short (length: 0.24 mm) but distinctly developed, with a sharp posterior edge. A
325 dense field of microtrichia is present on a transverse posterior metascutal concavity. The
326 metascutellum (scl3: Fig. 3B, D) attaches to the posterior metascutal margin. Postero-laterally
327 the postnotum (pn3: Fig. 3B, D) is inflected below the mesoscutum. Its lateral part forms a
328 triangle which is distinctly widening laterally. No metaphragma is developed. The oblique
329 metapleural suture (pls3: Fig. 3D) divides the metapleuron into the anterior metanepisternum
330 (aest3: Fig. 3D) and posterior metepimeron (ep3: Fig. 3D). The posterior edge of the narrow
331 metabasale (ba3: Fig. 3D) runs parallel to the metathoracic pleural wing process (pwp3: Fig.
332 3D) and comes close to the dorsal area of the metanepisternum ventrally. The metabasale of
333 other species in *Orectochilus* and Orectochilini is solidly attached to the metanepisternum
334 (Larsén 1966). The metasubalare (sa3: Fig. 3D) is very small (length: 0.02 mm, height: 0.02

335 mm) and embedded in the membranous area above the sclerotized metapleuron. The
336 metanepisternum is narrower than in *Orectogyrus* and *Gyretes* (Larsén 1966). The metepimeron
337 connects with the lateral metapostnotal edge postero-dorsally, and with a semicircular disc-like
338 element formed by the first abdominal pleuron.

339 The metaventrite (v3: Figs. 1B; 2B; 3D; 4A; 5A) reaches its maximum length at midline,
340 with narrow oblique lateral wings enclosed between the posterior margin of the mesocoxae and
341 the anterior margin of the metacoxae. The metakatepisternum is fused with the ventrite, without
342 a trace of a transverse ridge. The discrimen is also lacking, and the metatrochantin is not visible
343 externally. The metaventrite bears a narrow median process (width: 0.68 mm) fitting between
344 the postero-median mesocoxal edges. A visible cleft separates the dorsal metanepisternum from
345 the ventral metaventrite and metacoxa. The metacoxae (cx3: Figs. 1B; 2B, C; 3D; 4A; 5A) are
346 greatly enlarged compared to most other beetles and rectangular, extending far anterolaterad as
347 in other Orectochilini and Gyrimini (Hatch 1926; Larsén 1966). The oblique anterior margin is
348 fused with the posterior margin of the metaventrite. An anterolateral extension reaches into the
349 metathoracic lumen as a disc-like structure for muscle attachment. The fused median metacoxal
350 lamellae are longer than those of the mesocoxae. The connection area of the paired metacoxae
351 is visible as a median suture as in *Heterogyrus* and other Gyriminae (Larsén 1966). The narrow
352 metafurca (fu3: Fig. 4B) with paired parallel arms extends antero-dorsad from the metacoxal
353 lamella and almost reaches the mesofurca anteriorly. The hind legs as a whole are larger than
354 the middle legs. Their distal parts are similar, also forming shortened paddle-like structures for
355 swimming (metafemur length: 0.98 mm, width: 0.72 mm; length : width ratio = 1.4 : 1.0.
356 metatibia length: 1.11 mm, width: 0.79 mm; length : width ratio = 1.4 : 1.0). The internal walls
357 of the metatibiae (tib3: Figs. 1B; 2C; 5A) and the proximal tarsomere are also connected by
358 cuticular columnae (Larsén 1966). Tarsomere 4 is similar to its mesothoracic equivalent, also
359 forming a shovel-like structure with the proximal 3 tarsomeres. This structure is similar to the
360 condition found in other Orectochilini and Enhydrini (Larsén 1966; Beutel 1990).

361 The sclerotized anterior notal process (anp: Fig. 3B) is attached to the middle region of
362 the lateral metascutal margin. The elongate first axillary sclerite (1ax: Fig. 3B) is separated into
363 two parts by a suture in its middle section, and its antero-proximal part is close to the
364 basisubcostale (bsc: Fig. 3B). The narrow second axillary sclerite (2ax: Fig. 3B) is tightly
365 adjacent to the distal portion of the mesal margin of the first axillary sclerite. The third axillary
366 sclerite (3ax: Fig. 3B) bears three processes and a small proximal sclerite close to the posterior
367 part of the first axillary sclerite (length: 0.80 mm, width: 0.11 mm). The median plate (mp: Fig.

368 3B) is weakly sclerotized and not distinctly delimited from the membranous area of the wing
369 base. It is divided by a fold along its midline.

370 **Musculature** (Figs. 4; 5; Table 1): **M62** (IIvIm3) *M. metasterni primus*: O: posterior
371 surface of mesofurcal arm; I: anteriorly on metafurcal arm. **M67** (IIItpm2) *M. pleura-praealaris*:
372 O: metapleural wing process; I: metaprealar sclerite. **M69** (IIItpm3) *M. noto-basalaris*,
373 elongated triangular: O: lateral margin of metascutum; I: metabasalar. **M70** (IIItpm10) *M.*
374 *epimero-subalaris*, triangular, broader on metapostnotum, narrowing towards metasubalar: O:
375 postero-ventral margin of metapostnotum; I: metasubalar. **M71a** (IIItpm9) *M. pleura-alaris a*,
376 triangular, broader on metapleural ridge; narrowing towards third axillary sclerite: O: median
377 area of metapleural ridge; I: third axillary sclerite. **M71b** (IIItpm7) *M. pleura-alaris b*, elongated
378 triangular, broader on metanepisternum, narrowing towards third axillary sclerite: O: antero-
379 dorsal area of metanepisternum; I: third axillary sclerite. **M72** (IIIppm1) *M. sterno-episternalis*:
380 O: antero-dorsal area of metanepisternum; I: dorsal area of metaventrite. **M76** (IIIIdvm5) *M.*
381 *noto-coxalis posterior*, broad origin on metascutum, converging on a tendon inserted on
382 metacoxa: O: postero-lateral area of metascutum; I: postero-lateral metacoxal rim. **M84**
383 (IIIIdvm7) *M. noto-trochanteralis*: O: dorsal area of metascutum; I: large disc-shape apodeme
384 of metatrochanter. **M85** (IIIscm6) *M. furca-trochanteralis*: O: metafurcal arm; I: metatrochanter.
385 **M86** *M. coxa-trochanteralis medialis*, several bundles: O: anterior metacoxal rim and mesal
386 wall; I: metatrochanter. **M87** *M. coxa-trochanteralis lateralis*, two bundles, the anterior one
387 stronger with fibers converging medially, the posterior one shorter: O: lateral metacoxal rim; I:
388 metatrochanter. **Mx**, elongated conical, broader on first abdominal pleuron, narrowing towards
389 metacoxa: O: semicircular disc of first abdominal pleuron; I: postero-lateral metacoxal rim.

390 The metathoracic muscular apparatus metathorax comprises only 10 muscles (excl. **M86**
391 and **M87** as intrinsic metacoxal muscles, **Mx** as abdominal muscle), compared to 27 in a more
392 plesiomorphic pattern in other groups of Adephaga and in Polyphaga (Larsén 1966; Beutel and
393 Haas 2000) and 36 in the archostematan *Tetraphalerus bruchi* (Friedrich et al. 2009). Compared
394 to the coleopteran muscular pattern reported by Larsén (1966), **M60** (IIIIdlm1) *M. metanoti*
395 *primus*, **M61** (IIIIdlm2) *M. metanoti secundus*, **M63** (IIvIm5) *M. metasterni secundus*, **M64**
396 (IIIIdvm1) *M. dorsoventralis primus*, **M65** (IIIIdvm8) *M. dorsoventralis secundus*, **M66**
397 (IIIIdvm8) *M. dorsoventralis tertius*, **M68** (IIItpm6) *M. noto-pleuralis*, **M73** (IIIspm1) *M.*
398 *sterno-episternalis*, **M74** (IIIIdvm2) *M. noto-trochantinalis*, **M75** (IIIIdvm4) *M. noto-coxalis*
399 *anterior*, **M77** (IIIpcm4) *M. episterno-coxalis*, **M78** (IIIpcm3) *M. coxa-basalaris*, **M79**
400 (IIIIdvm6) *M. coxa-subalaris*, **M80** (IIscm7?) *M. sterno-coxalis*, **M81** (IIIscm1) *M. furca-*
401 *coxalis anterior*, **M82** (IIIscm4) *M. furca-coxalis lateralis* and **M83** (IIIscm2) *M. furca-coxalis*

402 posterior are absent. Only two dorsoventral muscles **M76** (III_{dvm}5) and **M84** (III_{dvm}7) are
403 present as indirect flight muscles. **M67** (III_{tpm}2), **M69** (III_{tpm}3), **M70** (III_{tpm}10) and **M71**
404 (III_{tpm}7 & 9) are present as direct flight muscles. **M85** (III_{scm}6) is present, but the other furca-
405 coxal muscles are absent.

406

407 **4. Discussion**

408 **4.1. Phylogenetic and evolutionary interpretations**

409 Even though Gyrinidae are arguably the “basal” sistergroup of the remaining adepagan
410 families and may have originated in the early Triassic or even the late Permian (Ponomarenko
411 1977; Beutel and Roughley 1988; Beutel et al. 2013; Baca et al. 2017), their morphology and
412 life habits are distinctly modified compared to the hypothetical groundplan of the suborder and
413 of Coleoptera (Beutel 1997; Beutel and Haas 2000; Friedrich et al. 2009). As is sometimes the
414 case with so-called “basal groups” (e.g. Monotremata in mammals or Struthionidae in birds;
415 Mickoleit 2004), the autapomorphies (Beutel 1989a, b, 1990; Miller and Bergsten 2012)
416 outweigh few preserved plesiomorphies, such as the lack of the torsion of aedeagus or the
417 retained intrinsic movability of the larval maxilla (Beutel and Roughley 1988). This mainly
418 reflects adaptations to surface swimming in the case of adults, and a preference for greater water
419 depths of the larvae, which are equipped with tracheal gills (Larsén 1966; Beutel and Roughley
420 1988).

421 The forelegs of Gyrinidae are long grasping devices suitable for seizing prey objects on
422 the water surface, apparently an autapomorphy of the family (Beutel 1989b). In contrast to most
423 other groups of Adepaga, the ventral procoxal joint is reduced in Gyrinidae, with the exception
424 of the “ancestral” *Spanglerogyrus* (Beutel 1989b), increasing the degrees of freedom at the leg
425 base. This character supports the monophyletic origin of the subfamilies Heterogyrinae
426 (*Heterogyrus*) and Gyrininae (Miller and Bergsten 2012; Beutel et al. 2017). Other features
427 characterizing this clade are the presence of a prothoracic proprioceptive organ with spatulate
428 setae (se: Fig. 3C) and the laterally compressed protarsi (tar1: Fig. 1B; 2A). In contrast to the
429 pterothoracic segments, the musculature of the prothorax is plesiomorphic, with a well-
430 developed set of neck muscles moving the head and normally developed leg muscles, similar
431 as in other groups of Coleoptera.

432 The mesothorax of Gyrinidae differs from all other Adepaga by the extensive and flat
433 mesoventrite, which does not articulate with the prosternal process. Phylogenetically this
434 character is ambiguous. Arguably it is a plesiomorphic trait compared with the short and
435 grooved mesoventrite found in the other aquatic families, and also in the terrestrial

436 Trachypachidae and Carabidae (partim) (Beutel and Roughley 1988; Beutel 1997). However,
437 this structure is apparently suitable for gliding on the surface film of the water and more likely
438 a secondarily acquired feature and autapomorphy of Gyrinidae.

439 The most conspicuous (and unique) synapomorphy of *Heterogyrus* and Gyrininae is the
440 transformation of the middle and hind legs into shortened and flattened paddle-like structures
441 (Fig. 2B, C), with a fan-shaped tarsus. The swimming lamellae (Larsén 1966), which do not
442 occur in any other aquatic group of beetles, create 52% of the propulsion force (Nachtigall
443 1961). These conditions are in contrast to the moderately modified middle and hind legs of
444 Dytiscidae and *Spanglerogyrus* (Beutel 1990; Nachtigall 1960), which are more or less
445 elongated and equipped with simple or feather-like swimming hairs, respectively. The paddle-
446 like middle and hind legs enable whirligig beetles to swim rapidly on the water surface, with a
447 frequency of the hind legs of about 60 strokes/sec and about 30/sec of the middle legs (Bott
448 1928; Nachtigall 1961). It was pointed out by Nachtigall (1961) that the paddle-like legs of
449 Gyrininae exceed the performance of comparable technical machines and form the best-known
450 thrust apparatus in the animal kingdom. The distal leg elements of *Gyrinus* investigated by
451 Nachtigall (1961) are plesiomorphic compared with those of Orectochilini and most Enhydrini.
452 The distal tarsomeres of Orectochilini and most enhydrine genera form a shovel-like structure
453 with the basal ones (Larsén 1966; Beutel 1990), which likely improves the efficiency.

454 An unusual apomorphy of Orectochilini is the far-reaching reduction of the metathoracic
455 muscular system. Compared with other groups of Neoptera, Coleoptera in general are
456 characterized by a simplified pterothoracic muscular system, probably linked with the strong
457 sclerotization without exposed membranes and reduced degrees of freedom, especially at the
458 leg bases (Beutel and Haas 2000; Friedrich et al. 2009). In contrast to more than 100
459 pterothoracic muscles suggested for the neopteran groundplan (Friedrich and Beutel 2008),
460 Larsén (1966) proposed 52 muscles as a plesiomorphic status of Coleoptera after a broad
461 investigation of Adephaga and Polyphaga. More recent studies suggest that more muscles are
462 present in the coleopteran groundplan (Beutel and Haas 2000; Friedrich et al. 2009). Sixty-nine
463 muscles were identified in *Tetraphalerus bruchi*, a species of Ommatidae in Archostemata,
464 which is currently recognized as an evolutionary relict (Friedrich et al. 2009). Other thoracic
465 plesiomorphies preserved in Ommatidae (and the closely related Cupedidae) are a transverse
466 ridge of the mesoventrite and exposed metatrochantins (Baehr 1975; Beutel and Haas 2000;
467 Friedrich et al. 2009). Within Orectochilini, only 22 pterothoracic muscles are preserved in *O.*
468 *villosus*, 17 in *Gyretes zimmermanni* Ochs, 1929 and 16 in *Orectogyrus ornaticollis* Aubé, 1838
469 (Table 1; Larsén 1954). Among them, 10 are preserved in the metathorax of *O. villosus* and 7

470 in the metathorax of the other two species examined by Larsén (1966). This is in agreement
471 with a general trend of decreasing complexity of the thoracic musculature in Pterygota and in
472 Coleoptera (Beutel and Haas 2000; Friedrich et al. 2009; Friedrich and Beutel 2010). The
473 metathoracic muscular number observed in Orectochilini are the lowest among 54 beetles
474 examined by Larsén (1966), also including flightless species if degenerated muscles are
475 considered as present (marked as 0 in Larsén 1966), and also less than those observed species
476 in more recent studies on the thorax of Coleoptera (Baehr 1975; Beutel 1986, 1988; Belkaceme
477 1991; Beutel and Komarek 2004; Friedrich and Beutel 2006). Derived skeletal features
478 correlated with the muscular reductions exclude the interpretation that conditions observed in
479 Orectochilini are due to slight intraspecific variation of the flight muscles. A conspicuous of
480 feature Orectochilini (and the enhydrine genera) is the medially shortened metanotum (Hatch
481 1925; Larsén 1966; Beutel 1990), which provides limited space for the dorsoventral muscles
482 and no suitable attachment areas for dorsal longitudinal muscles. The loss of the metaphragma
483 is apparently also linked with this modification.

484

485 **4.2. Functional interpretations of the locomotor apparatus (Fig. 6)**

486 Coleoptera are characterized by reduced degrees of freedom in their thoracic skeleton, and also
487 a distinctly reduced muscular system compared with other groups of Neoptera (Beutel and Haas
488 2000). The tendency to increase the efficiency and economy of the locomotor apparatus is
489 intensified in the non-archostematan suborders, notably in Polyphaga and Myxophaga (Beutel
490 and Haas 2000). However, a culminating point is reached in the adephagan tribe Orectochilini
491 of Gyridae, for instance *O. villosus*. Whrilig beetles in general have optimized surface
492 swimming and retained the capacity of flight with a distinctly reduced pterothoracic muscle set
493 (Larsén 1966).

494 The dorsal longitudinal muscles are completely missing in Orectochilini and other groups
495 of Gyridae (Larsén 1966), apparently linked with modifications of the metanotum (Beutel
496 1990). They are usually important elements of a flight apparatus operating with the neopteran
497 (and ephemeropteran) indirect mechanism (Brodsky 1994). The function of the metathoracic
498 dorsal longitudinal muscle **M60** (IIIdlm1) in Coleoptera is the longitudinal contraction of the
499 notum, which results in the initial depression of the wings with the first axillary sclerite (Figs.
500 6Ai, Aii; Brodsky 1994; Haas and Beutel 2001). This muscle is not only lacking in Orectochilini
501 but also in *Heterogyrus* and Gyridae (pers. obs. R.G. Beutel; Larsén 1966). The intrinsic
502 elasticity of the metanotum alone (Larsén 1966) does not provide a sufficient explanation of
503 the mechanism without adequate muscular control. Interestingly, the dorsal longitudinal

504 muscles are not only reduced in Gyrinidae, but also poorly developed in two distantly related
505 orders with posteromotorism, Orthoptera and Blattodea (Polyneoptera). In these cases, this is
506 compensated by the metabasalar muscles according to Brodsky (1994). In most examined
507 species of Gyrininae, the tergo-pleural muscle **M69** (IIItpm3) is present and the only muscle
508 attached to the metabasalar (Larsén 1966; Beutel 1990). Therefore, it is likely that this muscle
509 takes over the function of hind wing depression (Figs. 6Bi, Bii), with adduction and pronation
510 of the hind wing through the metabasalar as additional functions (Brodsky 1994). However,
511 **M69** (IIItpm3) is absent in most Orectochilini, and the metabasalar is solidly attached to the
512 metanepisternum in species of this tribe (Larsén 1966; Beutel 1990). We hypothesize that the
513 functions are taken over by the metapleural muscle **M72** (IIIppm1) which moves the sclerite,
514 with a cleft forming a joint between the metanepisternum, the metaventricle and the metacoxa
515 (Fig. 3D) (Larsén 1966: Orectochilini and *Dineutus*). **M72** (IIIppm1) is missing in *Gyrinus* and
516 *Aulonogyrus* (Larsén 1954, 1966; Beutel 1990), whereas **M69** (IIItpm3) is present in the species
517 of both genera. Under the control of the metabasalar, the basisubcostale also becomes
518 responsible for the depression (Brodsky 1994). The control of the first axillary sclerite is shifted
519 from the median notal process to the anterior notal process (Brodsky 1994), which is generally
520 preserved in Gyrinidae (Hatch 1926; Larsén 1966; Beutel 1990).

521 The large metathoracic dorso-ventral muscle **M84** (IIIIdvm7; in *O. villosus* length: 2.20
522 mm, width: 0.45 mm; length : width ratio = 4.9 : 1.0) of Gyrininae (Larsén 1966) must play a
523 dominant role as a levator of the hind wing, considering the absence of most other dorso-ventral
524 muscles (Fig. 6F; Larsén 1966). Additionally, this muscle is responsible for the backstroke of
525 the hind leg during swimming, as synergist of the large metacoxal muscle **M87** (Fig. 6F; Larsén
526 1966; in *O. villosus* length: 1.80 mm, width: 1.69 mm). During this activity, the hind wings and
527 associated elements of the flight apparatus are shielded and locked by the elytra, with the
528 mesonotal scutellar shield and the metanotal alacristae forming a combined elytral arresting
529 mechanism (Larsén 1966; Beutel 1990; Beutel and Haas 2000). The activity of **M84** (IIIIdvm7)
530 during flight is probably supported by another dorso-ventral muscle, **M76** (IIIIdvm5). However,
531 as this muscle is extremely slender (width 0.07 mm) compared with **M84** (IIIIdvm7), its effect
532 is probably minimal.

533 In the groundplan of Coleoptera and in most species examined, two muscles connect with
534 the metasubalar, the dorsal-ventral muscle **M79** (IIIIdvm6) and the tergo-pleural muscle **M70**
535 (IIItpm10) (Fig. 6C; Larsén 1954; Haas and Beutel 2001; Friedrich et al. 2009; Friedrich and
536 Beutel 2010). Due to the absence or reduction of **M79** (IIIIdvm6) in Gyrinidae except *Dineutus*
537 (Larsén 1966), its function has to be taken over by another muscle (Fig. 6D). It is conceivable

538 that the function of supination (Brodsky 1994) is taken over by **M70** (IIItpm10) in Orectochilini
539 and most other Gyrinidae (Larsén 1966).

540 It is noteworthy that the two bundles of the tergo-pleural muscle **M71** (IIItpm7 and 9) are
541 absent in the two orectochiline species *O. ornaticollis* and *G. zimmermanni* (Larsén 1966), as
542 in some other coleopteran species with reduced flight apparatus (Haas and Beutel 2001). As the
543 only muscle connected with the third axillary sclerite in Neoptera (Friedrich and Beutel 2008),
544 it is involved in at least three of the four stages of the wing stroke (Brodsky 1994), also initiating
545 the processes of unfolding and folding the wings (Brodsky 1994; Haas and Beutel 2001). We
546 cannot exclude the possibility that these two orectochiline species are flightless. However,
547 flight appears rather possible, as the hind wings and skeletal parts of their flight apparatus show
548 no observable traits of reduction compared with the other Gyrinidae (Larsén 1966). If indeed
549 individuals of these two species are able to fly, it is unclear how the loss of **M71** is compensated
550 for.

551 It was pointed out that elytral movement of beetles play a minor role in creating
552 propulsive forces during flight (Haas and Beutel 2001). Their obvious function is protecting the
553 hind wings at rest, also shielding and locking the flight apparatus during swimming in Gyrinidae
554 (Haas and Beutel 2001; Larsén 1966). Aside from this, they are probably also involved in flight
555 control, improving the maneuverability of beetles and directing the airflow to the hind wings
556 (Brodsky 1994). It was demonstrated for species of Orthoptera that the control of
557 posteromotoric flight is the most important function of the leathery forewings (Brodsky 1994).
558 The synchronous pronation and supination of coleopteran elytra during flight is probably not
559 only a passive movement (Haas and Beutel 2001), but also under the control of a series of
560 mesothoracic flight-related muscles associated with the articulatory processes of the elytra (elap:
561 Fig. 3A).

562 The pterothoracic segments of Orectochilini differ strongly from conditions observed in
563 other groups of Coleoptera (e.g. Larsén 1966; Belkaceme 1991; Beutel 1986, 1988; Beutel and
564 Komarek 2004, Friedrich et al. 2009), with a remarkable degree of reduction of the muscular
565 system. It is conceivable that this optimizes efficiency, especially in the context of dual
566 alternative functions of flight and swimming on the water surface. Future investigations with
567 biomechanical and physiological approaches may improve the understanding of the
568 Orectochilini locomotor system, and possibly inspire interesting applications in bionics in the
569 future.

570

571 **Acknowledgements**

572 We are very grateful to the editorial team, and to Dr. John Lawrence (Gympie, CSIRO Canberra)
573 and Prof. Dr. Darren Pollock (Eastern New Mexico University) for their valuable comments.
574 This project is financially supported by the European Union's Horizon 2020 research and
575 innovation program under the Marie Skłodowska-Curie grant agreement No. 642241.

576

577 **References**

- 578 Aubé C (1838) *Species général des Hydrocanthares et Gyriniens*. Méquignon Père et Fils, Paris.
- 579 Baca SM, Alana A, Gustafson GT, Short AEZ (2017) Ultraconserved elements show utility in
580 phylogenetic inference of Adephaga (Coleoptera) and suggest paraphyly of
581 "Hydradephaga". *Syst Entomol*. DOI: 10.1111/syen.12244.
- 582 Baehr M (1975) Skelett und Muskulatur des Thorax von *Priacma serrata* Leconte (Coleoptera,
583 Cupedidae). *Z Morph Tiere* **81**:55–101.
- 584 Belkaceme T (1991) Skelet und Muskulatur des Kopfes und Thorax von *Noterus laevis* Sturm.
585 Ein Beitrag zur Morphologie und Phylogenie der Noteridae (Coleoptera: Adephaga).
586 *Stuttg Beitr Naturk (A)* **462**:1–94.
- 587 Beutel RG (1986) Skelet und Muskulatur des Kopfes und Thorax von *Hygrobia tarda* (Herbst).
588 Ein Beitrag zur Klärung der phylogenetischen Beziehungen der Hydradephaga (Insecta:
589 Coleoptera). *Stuttg Beitr Naturk (A)* **388**:1–54.
- 590 Beutel RG (1988) Studies of the metathorax of the trout-stream beetle, *Amphizoa lecontei*
591 Matthews (Coleoptera: Amphizoidae): Contribution towards clarification of the
592 systematic position of Amphizoidae. *Int J Ins Morph Embryol* **17**:63–81.
- 593 Beutel RG (1989a) The head of *Spanglerogyrus albiventris* Folkerts (Coleoptera: Gyrinidae).
594 Contribution towards clarification of the phylogeny of Gyrinidae and Adephaga. *Zool Jb*
595 *Anat* **118**:431–461.
- 596 Beutel RG (1989b) The prothorax of *Spanglerogyrus albiventris* Folkerts, 1979 (Coleoptera,
597 Gyrinidae). Contribution towards clarification of the phylogeny of Gyrinidae. *Entomol*
598 *Basiliensia* **13**:151–173.
- 599 Beutel RG (1990) Phylogenetic analysis of the family Gyrinidae (Coleoptera) based on meso-
600 and metathoracic characters. *Quaest Ent* **26**:163–191.
- 601 Beutel RG (1997) Über Phylogense und Evolution der Coleoptera (Insecta), insbesondere der
602 Adephaga. *Verhandlungen des Naturwissenschaftlichen Vereins in Hamburg NF* **31**:1–
603 164.

604 Beutel RG, Haas F (2000) Phylogenetic relationships of the suborders of Coleoptera (Insecta).
605 Cladistics **16**:103–141.

606 Beutel RG, Komarek A (2004) Comparative study of thoracic structures of adults of
607 Hydrophiloidea and Histeroidea with phylogenetic implications (Coleoptera, Polyphaga).
608 Org Divers Evol **4**:1–34.

609 Beutel RG, Roughley RE (1988) On the systematic position of the family Gyrinidae
610 (Coleoptera: Adephaga). Z Zool Syst Evolut -Forsch **26**:380–400.

611 Beutel RG, Wang B, Tan JJ, Ge SQ, Ren D, Yang XK (2013) On the phylogeny and evolution
612 of Mesozoic and extant lineages of Adephaga (Coleoptera, Insecta). Cladistics **29**:147–
613 165.

614 Beutel RG, Yan E, Richter A, Büsse S, Miller KB, Yavorskaya M, Wipfler B (2017) The head
615 of *Heterogyrus milloti* (Coleoptera: Gyrinidae) and its phylogenetic implications. Arthr
616 Syst Phyl (in press).

617 Bott RH (1928) Beitrag zur Kenntnis von *Gyrinus natator substriatus* Steph. Z Morph Ökol
618 Tiere **10**:207–306.

619 Brinck P (1982) Results of the Austrian-Indian Hydrobiological Mission 1976 to the Andaman-
620 Islands: Part VIII: The whirligig beetles (Gyrinidae) of the Andaman Islands. Ann
621 Naturhist Mus Wien Ser B 225–227.

622 Brodsky AK (1994) The Evolution of Insect Flight, 2nd Ed. Oxford University Press, Oxford,
623 New York, Tokyo.

624 Folkerts GW (1979) *Spanglerogyrus albiventris*, a primitive new genus and species of
625 Gyrinidae (Coleoptera) from Alabama. Coleopt Bull **33**:1–8.

626 Friedrich F, Beutel RG (2006) The pterothoracic skeletomuscular system of Scirtoidea
627 (Coleoptera: Polyphaga) and its implications for the relationships of the beetle suborders.
628 J Zool Syst Evolut Res **44**:290–315.

629 Friedrich F, Beutel RG (2008) The thorax of *Zorotypus* (Hexapoda, Zoraptera) and a new
630 nomenclature for the musculature of Neoptera. Arthr Str Dev **37**:29–54.

631 Friedrich F, Beutel RG (2010) Goodbye Halteria? The thoracic morphology of Endopterygota
632 (Insecta) and its phylogenetic implications. Cladistics **26**:1–34.

633 Friedrich F, Farrell BD, Beutel RG (2009) The thoracic morphology of Archostemata and the
634 relationships of the extant suborders of Coleoptera (Hexapoda). Cladistics **24**:1–37.

635 Gyllenhal L. (1808) Insecta Suecica, Class I. Coleoptera sive Eleuterata. Tomus I [Pars 1]. F.
636 J. Leverentz, Scaris [Skara].

- 637 Haas F, Beutel RG (2001) Control of wing folding and the functional morphology of the wing
638 base in Coleoptera. *Zoology* **104**:81–168.
- 639 Hatch MH (1925) The phylogeny and phylogenetical tendencies of Gyrinidae. *Pap Mich Acad*
640 *Sci Arts Letts* **5**:429–467.
- 641 Hatch MH (1926) The morphology of Gyrinidae. *Pap Mich Acad Sci Arts Letts* **7**:311–350.
- 642 Heller KM (1913) Ein neuer Cupedidae. *Wien Entomol Ztg* **32**:235–237.
- 643 Koeth M, Friedrich F, Pohl H, Beutel RG (2012) The thoracic skeleton-muscular system of
644 *Mengenilla* (Strepsiptera: Mengenillidae) and its phylogenetic implications. *Arthropod*
645 *Struct Dev* **30**:1–13.
- 646 Larsén O (1954) Die Flugorgane der Gyrinidae (Coleoptera). *Opusc Entomol* **19**:74–214.
- 647 Larsén O (1966) On the morphology and function of the locomotor organs of the Gyrinidae and
648 other Coleoptera. *Opusc Entomol (Suppl)* **30**:1–241.
- 649 Legros C (1953) Un gyrinide nouveau de Madagascar (Coeloptera). *Naturaliste Malgache*
650 **5**(1):63-67.
- 651 Maki T (1936) Studies on the skeletal structure, musculature and nervous system of the Alder
652 Fly *Chauliodes formosanus* Petersen. *Mem Fac Sci Agric Taihoku Imp Univ* **16**:117–243.
- 653 McKenna DD, Wild AL, Kanda K, Bellamy CL, Beutel RG, Caterino MS, Farnum CW, Hawks
654 DC, Ivie MA, Jameson ML, Leschen RAB, Marvaldi AE, HcHugh JV, Newton AF,
655 Robertson JA, Thayer MK, Whiting MF, Lawrence JF, Ślipiński A, Maddison DR, Farrel
656 BD (2015) The beetle tree of life reveals Coleoptera survived end Permian mass
657 extinction to diversify during the Cretaceous terrestrial revolution. *Syst Entomol* **40**:835–
658 880.
- 659 Mickoleit, G. (2004) *Phylogenetische Systematik der Wirbeltiere*. Verlag Dr. Friedrich Pfeil,
660 München.
- 661 Miller KB, Bergsten J (2012) Phylogeny and classification of whirligig beetles (Coleoptera:
662 Gyrinidae): relaxed-clock model outperforms parsimony and time-free Bayesian analyses.
663 *Syst Entomol* **37**:706–746.
- 664 Müller OF (1776) *Zoologie Danicae Prodromus seu Animalium Daniae et Norvegiae*
665 *indigenarum characteres, nomina, et synonyma imprimis popularium*. Hafniae, Typiis
666 Hallageriis.
- 667 Nachtigall W (1960) Über Kinematik, Dynamik und Energetik des Schwimmens einheimischer
668 Dytisciden. Zugleich ein Beitrag zur Anwendung von Kurzzeiphotographie und
669 Hochfrequenzkinematographie auf biologische Probleme. *Z Vergl Phys* **43**:48–118.

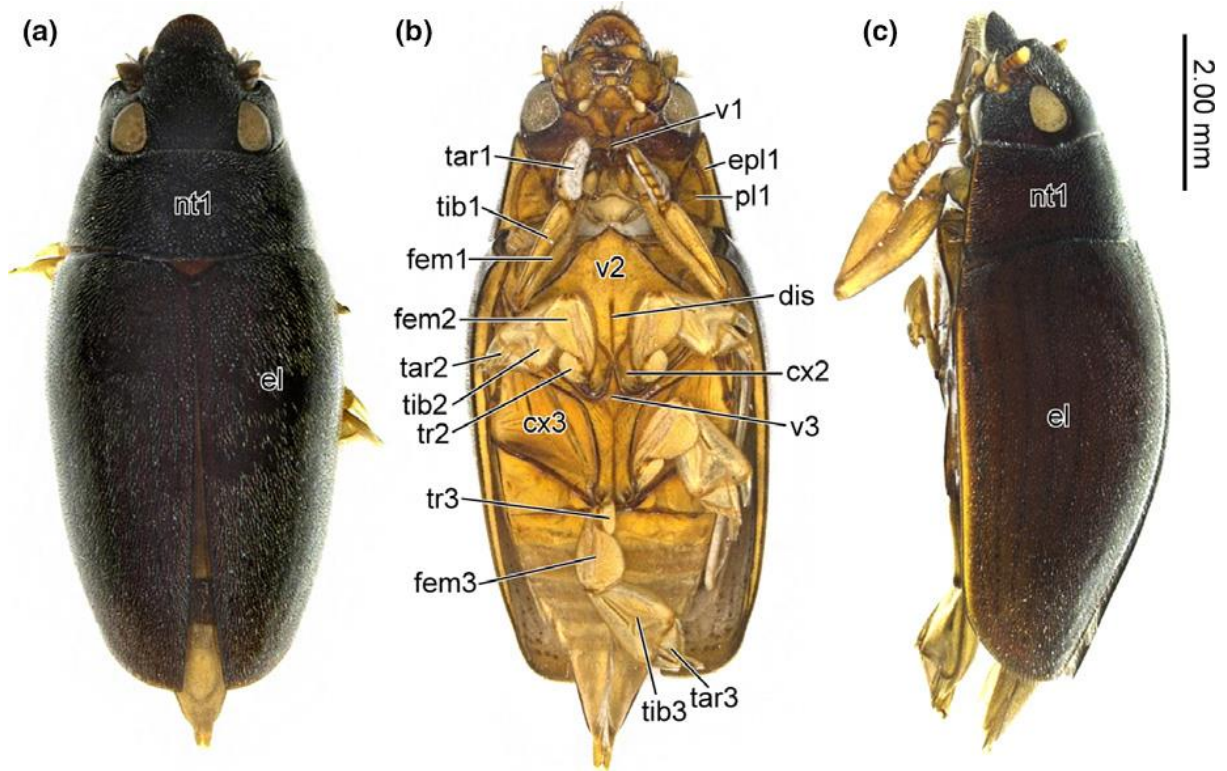
- 670 Nachtigall W (1961) Funktionelle Morphologie, Kinematik und Hydromechanik des
671 Ruderapparates von *Gyrinus*. *Z Vergl Phys* **45**:193–226.
- 672 Ochs G (1929) The present status of knowledge about Chinese Gyrinidae. *Lingnan Sci J* **7**:715–
673 720.
- 674 Ochs G (1966) Beiträge zur Kenntnis der Nepalischen Gyriniden (Col.). In *Khumbu Himal-*
675 *Ergebnisse des Forschungsunternehmens Nepal Himalaya*. Springer, Berlin, Heidelberg
676 243–246.
- 677 Omer-Cooper J (1934) Notes on the Gyrinidae. *Odbitka Arch Hydrobiol Rybactwa* **8**:1–26.
- 678 Ponomarenko AG (1977) Suborder Adephaga. *Tr Paleont Inst Akad Nauk SSSR* **161**:1–104.
679 [in Russian]
- 680
- 681

682 **Table 1: The Thoracic Musculature of Orectochilini**
683 (Muscular nomenclatures from Larsén (1954) and Friedrich and Beutel (2008) are listed
684 respectively in the first and second rows due to homology (Friedrich et al. 2009). Here we revise
685 M38 is homologous as Ispm5 instead of Ispm6, according to the origin and insertion of this
686 muscle in the same side of the insect body. Muscle present is represented with “+” in green,
687 absent with “-” in orange, unsure with “?” or “/” in yellow.)

Larsén 1954	Friedrich & Beutel 2008	<i>Orectochilus villosus</i>	<i>Orectogyrus ornatocollis</i>	<i>Gyetes zimmermanni</i>
Prothorax				
M1	ldlm2	+	+	-
M2	ldlm1	+	+	+
M3	ldlm3	+	+	+
M4	ldlm5	-	-	-
M5	lvlm3	+	+	+
M6	lvlm1	+	+	+
M7	ldvm6	+	+	+
M8	ldvm8	-	-	-
M9	ldvm5	-	-	-
M10	ldvm2/3	+	+	+
M11	ldvm10	+	+	+
M12	ltpm3?	-	-	-
M13	ltpm6	+	+	+
M14	ldvm13	+	+	+
M15	ldvm16/17	+	+	+
M16	lpcm4	+	+	+
M17	lpcm8	-	-	-
M18	lscm1	-	-	-
M19	lscm2	-	-	-
M20	lpcm8	+	+	+
M21	/	+	/	/
M22	/	+	/	/
Mesothorax				
M28	lldlm1	+	+	+
M29	lldlm2	-	-	-
M30	lvlm7	+	+	+
M31	lvlm9	-	+	+
M32	lldvm8	-	-	-
M33	lltpm2	+	+	-
M34?/35	lltpm10	-	-	-
M36a	lltpm9	-	-	-
M36b	lltpm7	-	-	-
M37	lspm2	-	-	-
M38	lspm5	+	+	+
M39	lldvm2	-	-	-
M40	lldvm4/5	+	-	-
M41	llpcm4	+	-	+
M42	llpcm3	-	-	-
M43	lldvm6	+	-	-
M44	llscm1	-	-	-
M45	llscm4	-	-	-
M46	llscm2	+	-	+
M47	lldvm7	+	+	+
M48	llpcm6	+	+	+
M49	/	-	-	-
M50	llpcm5	-	-	-
M51	?	+	+	+
M52	llscm6	+	+	+
M53	/	+	/	/
M54	/	+	/	/

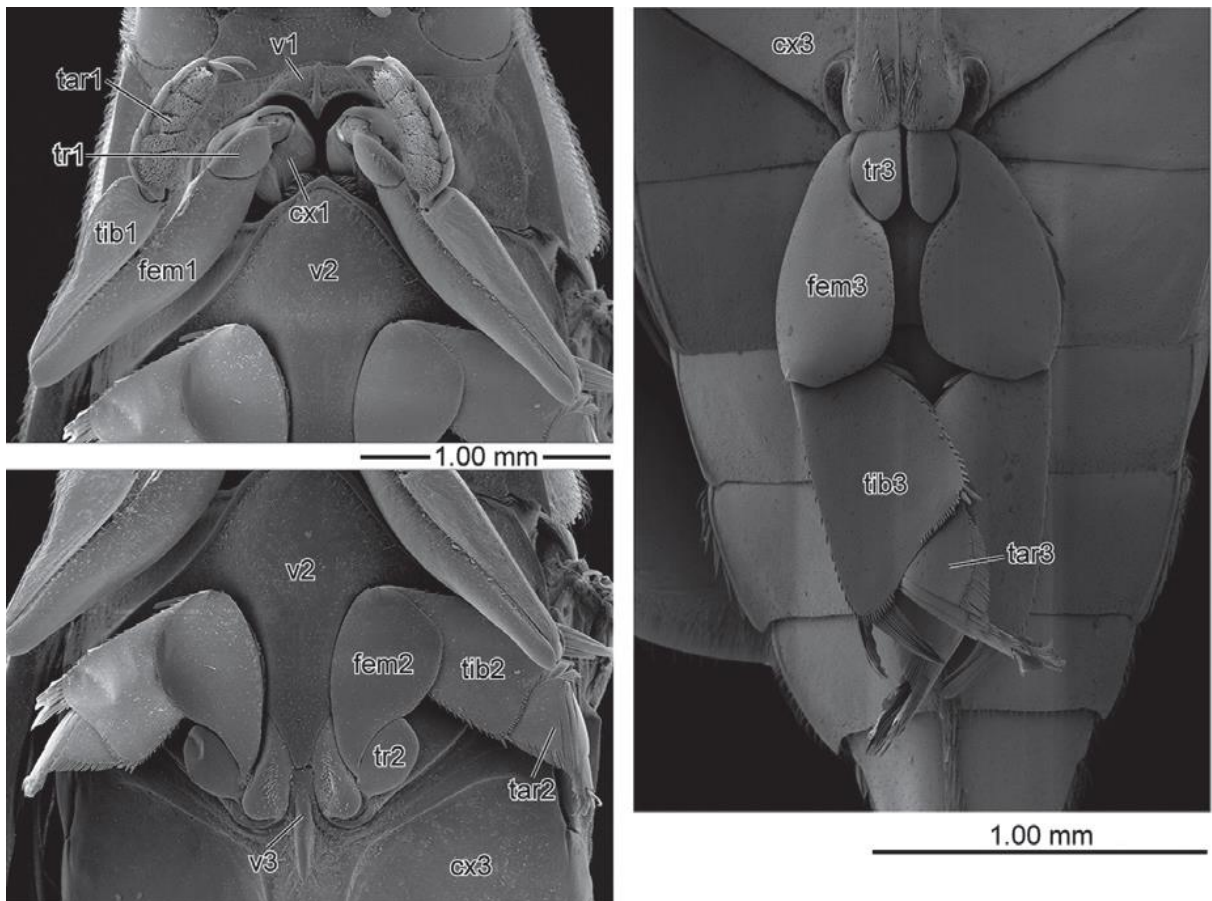
688
689
690
691
692
693
694
695
696
697
698
699
700
701
702
703
704
705
706
707
708
709
710
711
712
713
714
715
716
717
718
719
720
721

Metathorax				
M60	IIldlm1	-	-	-
M61	IIldlm2	-	-	-
M62	IIvlm3	+	+	+
M63	IIvlm5	-	-	-
M64	IIldvm1	-	-	-
M65	IIldvm8	-	-	-
M66	IIldvm8	-	-	-
M67	IIltpm2	+	+	+
M68	IIltpm6	-	-	-
M69	IIltpm3	+	-	-
M70	IIltpm10	+	+	+
M71a	IIltpm9	+	-	-
M71b	IIltpm7	+	-	-
M72	IIlppm1	+	+	+
M73	IIlspm1	-	-	-
M74	IIldvm2	-	-	-
M75	IIldvm4	-	-	-
M76	IIldvm5	+	+	+
M77	IIlpcm4	-	-	-
M78	IIlpcm3	-	-	-
M79	IIldvm6	-	-	-
M80	IIlscm7?	-	-	-
M81	IIlscm1	-	-	-
M82	IIlscm4	-	-	-
M83	IIlscm2	-	-	-
M84	IIldvm7	+	+	+
M85	IIlscm6	+	+	+
M86	/	+	/	/
M87	/	+	/	/
Mx	/	+	/	/



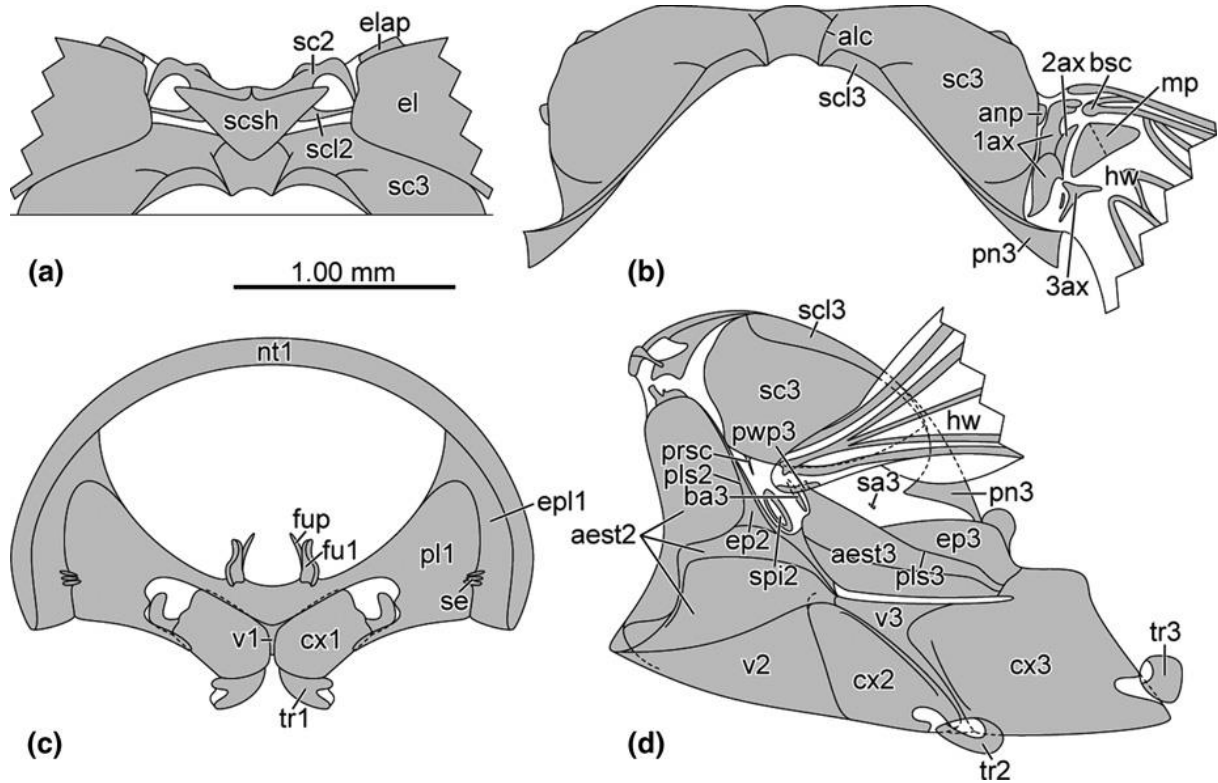
722
723
724
725

Fig. 1. *Orectochilus villosus*, digital photographs, male habitus. **A:** dorsal view; **B:** ventral view; **C:** lateral view.

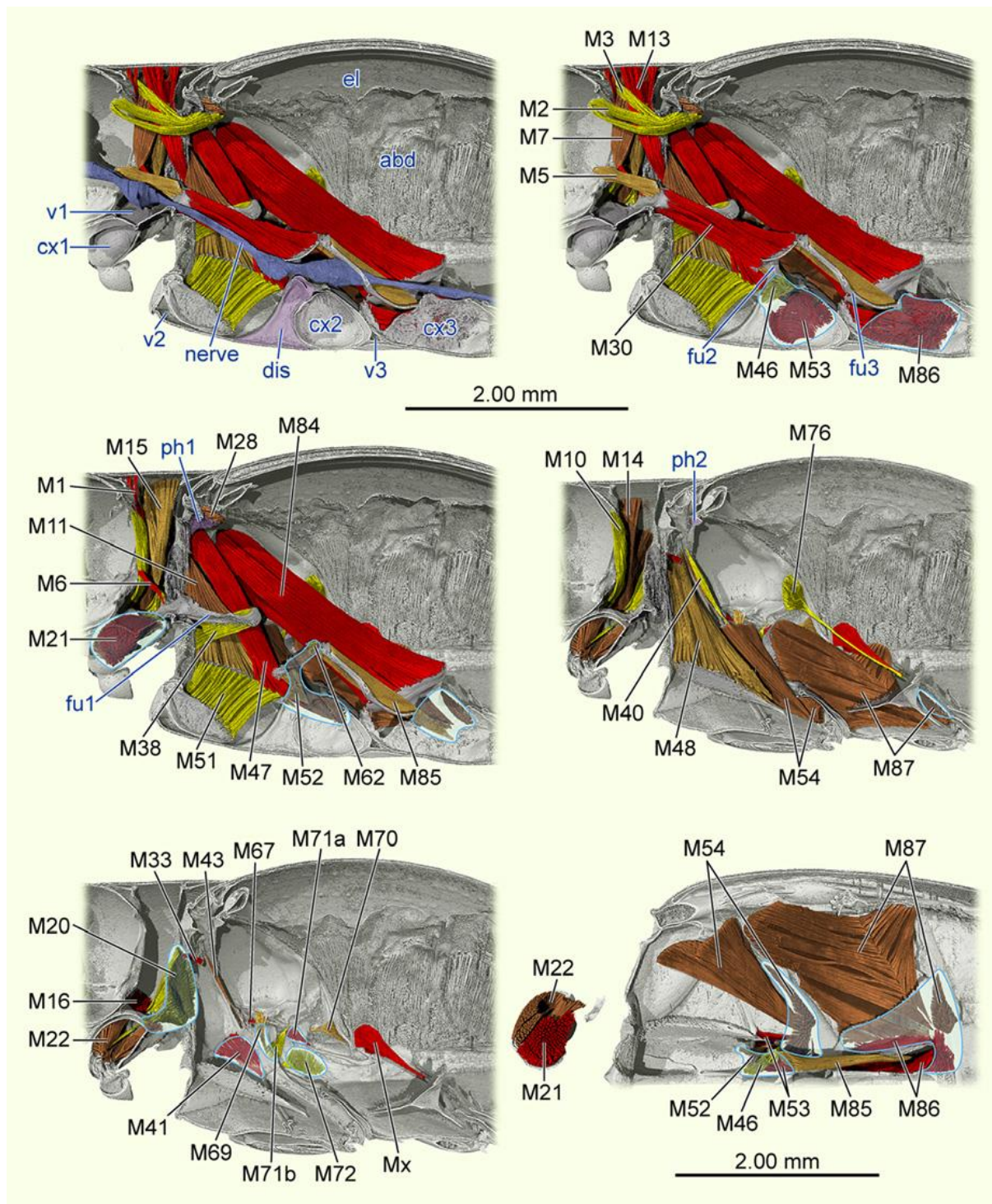


726

727 **Fig. 2.** *Orectochilus villosus*, SEM micrographs, male legs. **A:** fore leg; **B:** mid leg; **C:** hind
 728 leg.
 729

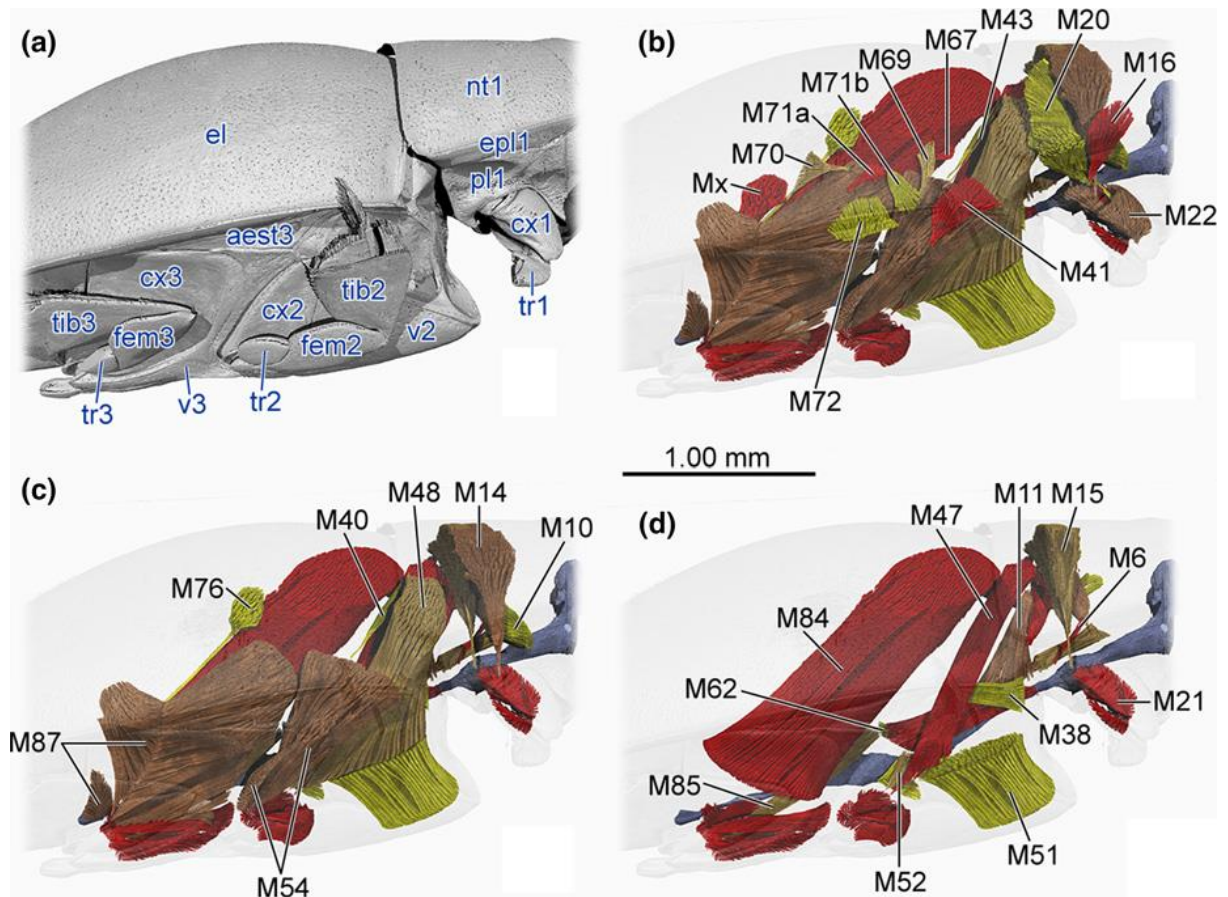


730
 731 **Fig. 3.** *Orectochilus villosus*, line drawing, thoracic skeleton. **A:** dorsal view of mesothorax; **B:**
 732 dorsal view of metathorax; **C:** posterior view of prothorax; **D:** lateral view of pterothorax.
 733



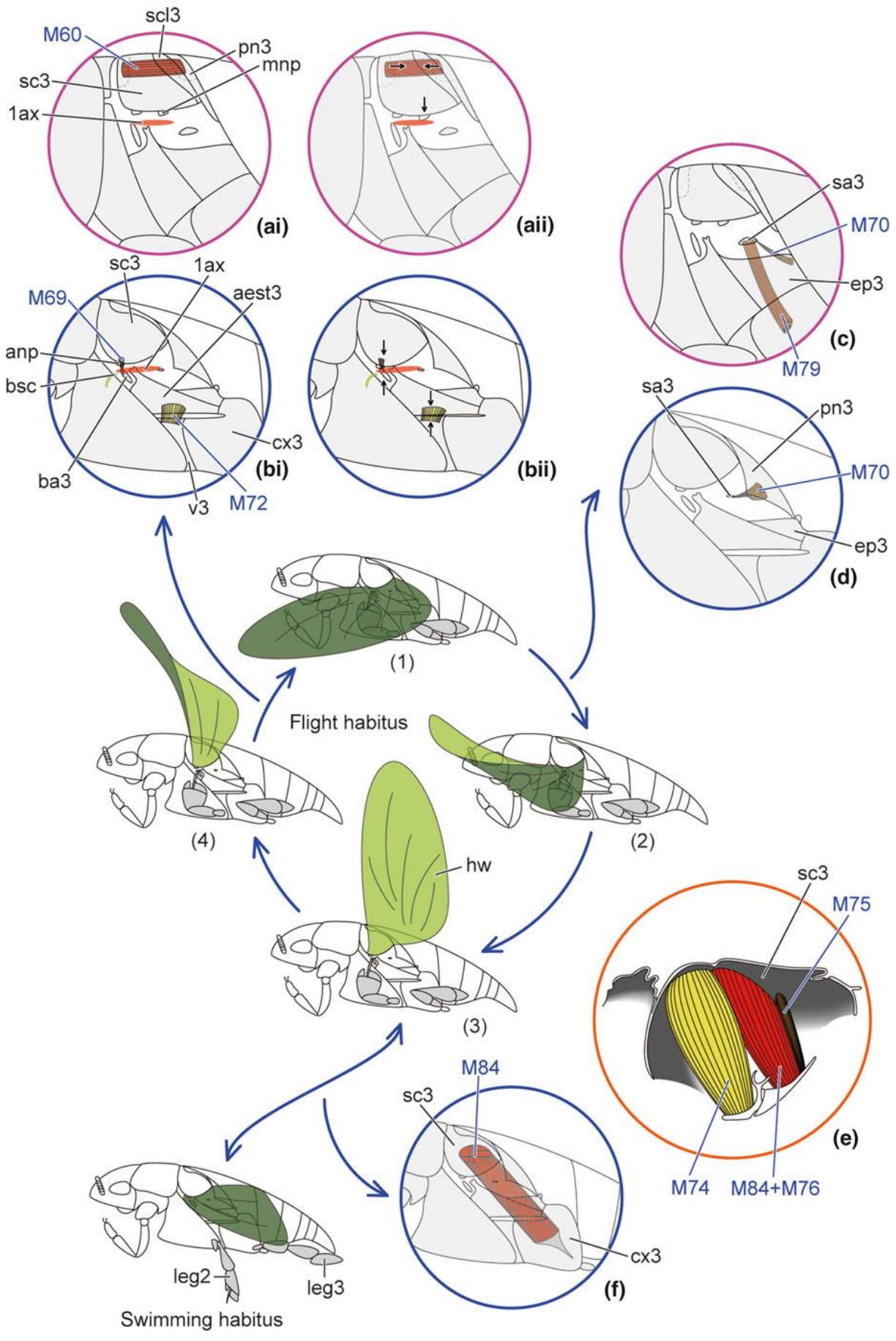
734
 735
 736
 737
 738
 739
 740
 741

Fig. 4. *Orectochilus villosus*, 3D-reconstruction, thoracic endoskeleton and muscles. Skeletal structures in blue lines rendered transparent to show muscles behind them. Skeletal structures labeled in blue, muscles in black. **A-E:** lateral view, dis and ph1/2 in pink; **F:** dorsal view, coxal muscles. **Scale bars:** upper 2.00 mm for **A-E**, lower 2.00 mm for **F**.



742
 743
 744
 745
 746

Fig. 5. *Orectochilus villosus*, 3D-reconstruction, thoracic skeleton and muscles. Skeletal structures labeled in blue, muscles in black. **A:** lateral view, exoskeleton; **B-D:** lateral view, skeleton transparent.



748 **Fig. 6.** Schematic diagram for functional interpretation. The insect wing stroke can be divided
749 into 4 distinct stages (Brodsky 1994): **(1)** depression and turning forward; **(2)** turning backward
750 and beginning supination; **(3)** elevation and end of supination; **(4)** pronation. In Gyrinidae, the
751 mid- and hind legs (leg2, 3) are laid close to the body during flight (Larsén 1966), and
752 alternatively extended and flexed during swimming (Nachtigall 1961). Elytra omitted. **Ai, Aii:**
753 **M60** (IIIIdlm1) initiates depression in generalized Coleoptera; **Bi, Bii:** either **M69** (IIItpm3) or
754 **M72** (IIIppm1) initiate depression in Gyrinidae; **C:** both **M70** (IIItpm10) and **M79** (IIIIdvm6)
755 control supination in generalized Coleoptera; **D:** only **M70** (IIItpm10) controls supination in
756 Gyrinidae; **E:** the large metacoxal muscles nearly form a single compact unit in the cricket
757 *Gryllus bimaculatus* (redrawn from Brodsky 1994: fig. 7.13a(ii)); **F:** extremely large **M84**
758 (IIIIdvm7) controls both hind wing elevation and hind leg backstroke.
759